MIRANDA'S POLYGONAL IMPACT CRATERS SUPPORT LONG-LIVED TECTONIC ACTIVITY. Richard. J. Cartwright[1,2] and Chloe B. Beddingfield[1,2], [1]The Carl Sagan Center at the SETI Institute, 189 Bernardo Ave., Suite 200 Mountain View, CA 94043, [2]NASA Ames Research Center, Building 245, Moffett Blvd. Mountain View, CA 94035 (chloe.b.beddingfield@nasa.gov).

Introduction: The mid-sized "classical" Uranian moon Miranda displays abundant evidence for tectonic resurfacing. Miranda's surface is punctuated by the polygonal shaped coronae and the Global Rift System (*e.g.*, [1-3]). Elsinore, Arden, and Inverness Coronae, are located near the center of Miranda's trailing, leading, and southern hemisphere, respectively. Previous work shows that Miranda's coronae are at least partially tectonic in origin (*e.g.*, [3-6]).

The centers of all three coronae are smoother and less cratered than the surrounding terrains, suggesting a younger age [2-3,7]. Elsinore is ancient (~2-3.5 Gyr), whereas Arden and Inverness are estimated to be younger (~0.1-1 Gyr), with Arden likely being older than Inverness based on its slightly higher crater density [7]. Miranda also displays an ancient cratered terrain, with an estimated age of ~2 to > 3.5 Gyr [7]. The canyons and fractures that comprise the Global Rift System likely formed over a long period of time that encompassed, and continued after, the coronae formation period(s) [3].

Along with examples of circular impact craters (CICs), polygonal impact craters (PICs) are also present on Miranda. PICs exhibit at least one straight rim segment (*e.g.*, [8-11]). The only known formation mechanism for PICs is pre-existing, sub-vertical extensional and strike-slip structures within the target material (*e.g.*, [12-13]). Contractional features could also influence crater morphologies, but the relationship between contractional features and PICs is still poorly understood. PICs have been identified on all of the terrestrial planets and numerous small bodies including icy satellites (*e.g.*, [11,14]).

Data and Methods: We analyzed 49 impact craters identified in Voyager 2 Imaging Science System (ISS) data [15]. Processing of all ISS data was done using the USGS Integrated Software for Imagers and Spectrometers3 (ISIS3). Illumination geometry does not have a strong effect on the identification of PICs [16], and so we were able to use all available ISS images of Miranda. We projected these images to the center of each crater to maximize the accuracy of our geometry measurements. Craters overprinted by other craters, and craters cut by faults and other features, were not analyzed. Additionally, crater chains/clusters and craters smaller than ~10 times the image resolution were also excluded from our analysis.

We manually traced the rims of all analyzed craters, normalized each traced rim, and then broke them into segments of equal length. We then calculated the azimuth of each rim segment and generated rose diagrams for each crater's azimuth distribution (Fig. 1).

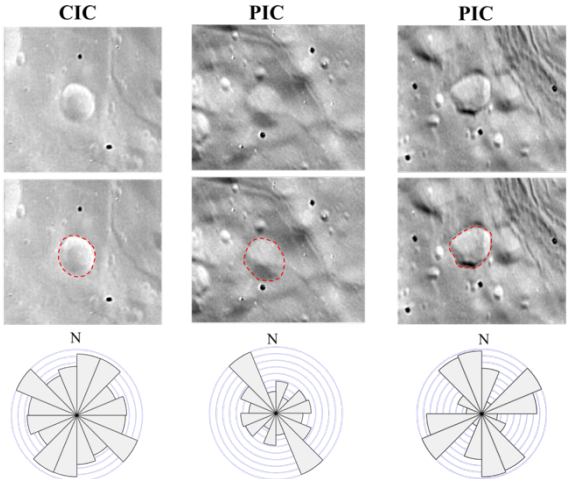

Fig. 1: Examples of different types of craters on Miranda, including a CIC (left column) and PICs with unimodal and bimodal orientations (middle and right columns, respectively).

To identify PICs, we tested for uniform azimuth distributions, using the Pearson's Chi-squared test. Our null hypothesis was that the azimuth distribution for each crater is uniform (*i.e.*, consistent with CICs), and we set the associated p-value to 0.05. Craters that reject this null hypothesis were identified as PICs. Next, we determined whether identified PICs reflect one or multiple straight rim segments using a Dip test. We then identified the prominent unimodal (single straight rim segment) or bimodal orientations for each PIC (Fig. 1) (the Dip test cannot assess significance beyond two modes). Thus, each PIC we analyzed could reflect one or two fracture sets with different azimuths.

Results: Of the 49 craters we analyzed, fourteen were classified as PICs [17]. Nine of the fourteen PICs are on Miranda's trailing hemisphere, four of which are located on Elsinore's bounding terrain and the other five are on the surrounding cratered terrain. One other crater might be associated with Elsinore but is somewhat distal from this coronae. Another PIC is proximal to Arden and the other three are associated with Verona Rupes and the Global Rift System.

The PICs on, and proximal to, Elsinore's bounding terrain display prominent NW-SE orientations, likely resulting from localized fracture sets (hereon called the

NW fractures) [17]. Utilizing crosscutting relationships, we determined that the NW fractures overprint Elsinore. Additionally, based on the locations of PICs displaying NW-SE orientations, the NW fractures appear widespread, spanning much of Elsinore and the adjacent cratered terrain, reaching locations on Miranda's Anti-Uranus hemisphere (Fig. 2). The orientation of the NW fracture system is consistent with subtle, but visible, fractures that overprint Elsinore. The PICs associated with Verona Rupes show prominent N-S rim orientations, consistent with the surrounding fractures. The PIC near Arden exhibits a N-S orientation that appears to be consistent with the nearby boundary of Arden. The PIC on Miranda's Anti-Uranus hemisphere displays a NW orientation, possibly associated with the NW fractures that overprint Elsinore.

Discussion: The PICs that overprint the NW fractures include examples of both fresh (*i.e.*, non-mantled) and subdued (*i.e.*, mantled) craters [17]. The subdued crater population is one of the oldest features on Miranda and is older than the fresh crater population [3,7]. None of the PICs or CICs identified on Elsinore are subdued craters, indicating that Elsinore (as well as the younger Arden and Inverness Coronae) formed after the subdued crater population.

Thus, the process that initiated the NW fractures predates the formation of the coronae and the subdued and fresh crater populations. The NW fractures continued to develop over an extended period of time, perhaps episodically, and was likely re-activated, forming the subtle fractures observed overprinting Elsinore. Given the large spatial extent of the NW fractures, and the long temporal baseline over which this fracture system was active, the stress event responsible for forming the NW fractures was likely hemispherical or global in scale, such as true polar wander [17]. Miranda has therefore undergone multiple episodes of resurfacing, likely spanning large swaths of its geologic history.

Analogous to Miranda, the Saturnian moon Enceladus exhibits complex and widespread features that are at least partially tectonic in origin (*e.g.*, [18]). These two satellites are comparable in size and have ancient cratered terrains with examples of fresh and subdued craters. Both moons have three large regions of resurfacing, centered on their leading and trailing hemispheres and near their south poles. Furthermore, both moons' surface compositions display hints of NH_3-bearing species (*e.g.*, [19-20]), which are efficient antifreezes in liquid water. This constituent is known to originate in the interior of Enceladus due to its presence in plume material emanating from its South Polar Terrain [21]. If the NH_3-bearing material hinted at on Miranda also originated in its interior, then Miranda could still be geologically active, either now or in the recent past, making it a candidate ocean world.

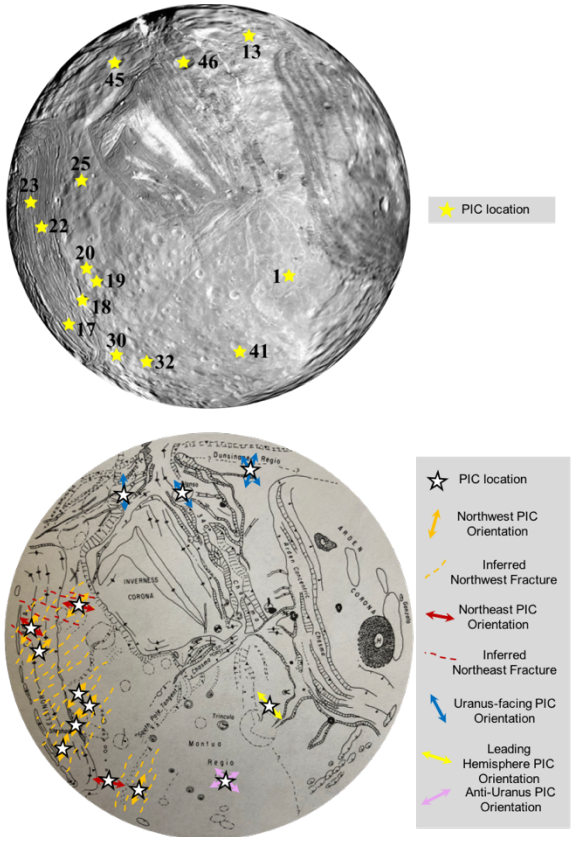

Fig. 2: Voyager 2 ISS image mosaic shown in a south polar stereographic projection with locations of the 14 PICs identified in this study (top). Published geologic map of Miranda [3] showing the locations and orientations of the prominent PIC rim segments.

References: [1] Smith et al., 1986. *Science* 233, p.43. [2] Croft and Soderblom, 1991. In *Uranus,* U.A.P., p.561. [3] Greenberg et al. 1991. In *Uranus*, U.A.P. p.693. [4] Schenk, 1991. *J.G.R.* 96, p.1887. [5] Pappalardo et al., 1997. *J.G.R.* 102, p. 13369. [6] Beddingfield et al., 2015. *Icarus* 247, p.35. [7] Zahnle et al., 2003. *Icarus* 163, p.263. [8] Fielder, 1961, *P.&S.S.*, 8, p.1. [9] Shoemaker, 1962, *Physics and Astro. of the Moon*, p.283. [10] Ohman et al., 2005. In *Impact Tectonics*, Springer, p.131. [11] Beddingfield et al., 2016. *Icarus* 274, p.163. [12] Schultz, 1976, *Interpret. based on lunar orbiter photo*. U.T.P. [13] Ohman, 2009. *Res Terrae, Ser.A*, 28 [14] Melosh and Dzurisin, 1978. *Icarus* 35, p.227. [15] https://pds-imaging.jpl.nasa.gov [16] Ohman et al., 2006. *M&P.S.* 41. P.1163. [17] Beddingfield and Cartwright, 2020. *Icarus* [In Press]. [18] Porco et al. 2006. *Science* 311, p.1393. [19] Bauer et al., 2002. *Icarus* 158, p.178-190. [20] Emery et al., 2005. *A&A* 435, p.353-362. [21] Waite et al., 2009. *Nature* 460, p.487.